Experimental study of the strength and crushing of unsaturated spherical particles

Caicedo B., Cacique A. & Contreras C.
Department of Civil and Environmental Engineering University of los Andes, Carrera 1 N° 18 A 10, Bogota, Colombia.
Vallejo L.E.
Department of Civil and Environmental Engineering, University of Pittsburgh, Pittsburgh PA 15261, USA

ABSTRACT
An experimental research program has been undertaken to investigate the behaviour of spherical particles under compression. Some theoretical aspects are revisited and then the experimental program is presented. The results show that Hertz theory is not the most appropriate theory to describe the contact behaviour between particles. Also the strength and the grain size distribution after crushing are presented.

RÉSUMÉ
Un programa experimental se ha llevado a cabo con el fin de investigar el comportamiento de partículas esféricas en compresión. Se presentan algunos aspectos teóricos y luego se describe el programa experimental. Los resultados muestran que la teoría de Hertz no es aplicable para describir el contacto entre partículas granulares. También se presenta en este artículo la resistencia de las partículas y su distribución granulométrica después de la falla.

1 INTRODUCTION

Granular materials forming part of geotechnical structures like flexible pavements, or embankments experience abrasion and crushing as a result of static and dynamic loads applied during the compaction process or during operation. Abrasion takes place when the sharp corners of the particles of gravel are removed as a result of compressive and shear loads. As a result of abrasion, the particles change in shape. Crushing is caused by the fragmentation of the particles into a mixture of many small particles of varying sizes.

Numerical models based on the discrete element technique using cylindrical or spherical particles has been used to simulate the crushing of granular materials; however to move forward these models in to more realistic conditions it is necessary to provide data of the behavior of actual grains particles. Particularly there are few experimental results about the plastic strain on the contacts of the particles, the effect of the water content on their strength, and the grain size distribution after crushing.

In this study, the behavior of spherical particles under monotonic and cyclic loading is analyzed. The laboratory component of this study involves unsaturated spheres of different diameter made of a mixture of sand and cement and prepared at different strengths (cement percentage). The spheres are immersed in an atmosphere having controlled hygrometry in order to control their suction level; afterwards the spheres are subjected to either monotonic or cyclic loading. During the tests the load and strain are recorded as well as the grain size distribution after crushing. The effect of the water content and the suction level on the strength of the spheres and on the stiffness of the contacts are highlighted.

The results of this study provide new experimental data to be implemented in the discrete element models to evaluate crushing of granular materials in a more realistic way.

2 FUNDAMENTALS OF STRESS, STRAIN AND STRENGHT IN GRANULAR MATERIALS

Experimental studies of granular material using photoelasticity were extensively led from the very beginning of soil mechanics studies, these studies are well described in literature, Dantu (1957), Allersma (1987, 2001), Dresher (1976), Dresher et al. (1972). Also numerical studies using discrete element models, Cundall and Strack (1979), have shown that the stress in granular materials is carried by force chains which load some particles, leaving other rather lightly loaded. This localization of strains and stresses is essential in the behavior of granular materials.

More recent developments in discrete element models includes particle damage, mainly crushing, during loading, Cheng at al. (2003), Harireche and McDowell (2003), Jensen et al. (2001), Mc Dowel and Harireche (2002), Lobo-Guerrero and Vallejo (2005a, 2005b, 2006). However despite of the huge developments on the modeling of granular materials there are several basic, but still opened questions, concerning the particles behavior at the contact between grains, the development of plastic deformation and the formation of new particles after crushing.

2.1 Elastic contact of spherical particles under normal loading: Hertz theory

Most of DEM simulations use laws for elastic contact of two spherical particles in the normal direction; these laws are based on Hertz theory, Hertz (1882). In the case of two spheres: sphere (i) and sphere (j), in contact with

each other as shown in Figure 1, subjected to a normal contact force P, and having the following characteristics: R_i and R_j are the radii of sphere (i) and sphere (j), respectively; the material properties of sphere (i) are denoted by E_i for the Young's modulus and by ν_i for the Poisson's ratio; similarly for sphere (j).

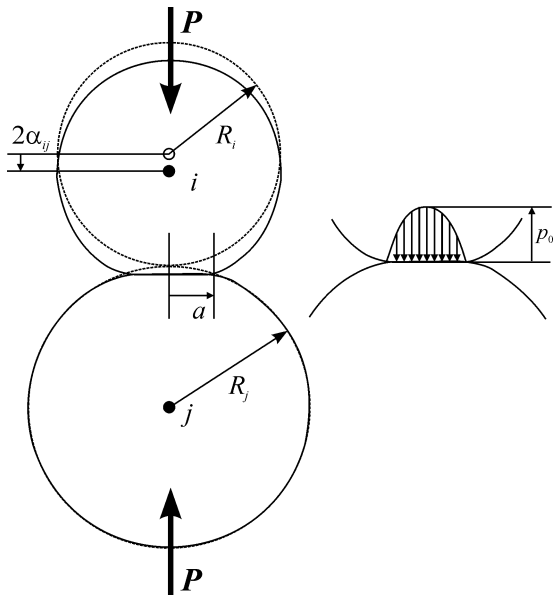

Figure 1. Two spheres in contact in the normal direction.

The equivalent Young's modulus E^* for the two spheres is defined as follows, Vu-Quoc and Zhang (1999):

$$E^* = \left[\frac{1-\nu_i^2}{E_i} - \frac{1-\nu_j^2}{E_j} \right] \qquad [1]$$

The relative radius R* of contact curvature is:

$$R^* = \left[\frac{1}{R_i} + \frac{1}{R_j} \right]^{-1} \qquad [2]$$

The radius of the circular contact area after Hertz is:

$$a = \left(\frac{3PR^*}{4E^*} \right)^{1/3} \qquad [3]$$

The normal displacement, $2\alpha_{ij}$, between the centers of both spheres is:

$$2\alpha_{ij} = \frac{a^2}{R^*} = \left[\frac{9P^2}{16R^*(E^*)^2} \right] \qquad [4]$$

According to Hertz, the distribution of normal stress, p, on the contact area is:

$$p = p_0 \left[1 - \left(\frac{r}{a} \right)^2 \right]^{1/2} \qquad [5]$$

Where r is the distance from the centre of the contact area, and p_0 is the maximum normal pressure at the centre of the contact area; p_0 is given by:

$$p_0 = \frac{3P}{2\pi a^2} = \left[\frac{6P(E^*)^2}{\pi^3 (R^*)^2} \right]^{1/3} \qquad [6]$$

The experimental component of this paper focuses on spheres of identical size, then in this case $R=R_i=R_j$, $E=E_i=E_j$, $\nu=\nu_i=\nu_j$, then the equivalent Young modulus and the radius of relative contact curvature are:

$$E^* = \frac{E}{2(1-\nu^2)} \quad \text{and} \quad R^* = \frac{1}{2}R \qquad [7]$$

Consequently the radius of the contact area is

$$a = \left[\frac{3PR(1-\nu^2)}{4E} \right]^{\frac{1}{3}} \qquad [8]$$

And the normal displacement α_{ij} is:

$$\alpha_{ij} = \frac{a^2}{R} = \left[\frac{9P^2(1-\nu^2)^2}{16RE^2} \right]^{\frac{1}{3}} \qquad [9]$$

2.2 Models for elastoplastic contact

Different methods has been proposed to account for the plastic strains appearing at the contact between particles when loading above a predefined elastic limit: Walton and Braun (1986), Thornthon (1997), and Vu Quoc and Zhang (1999).

The approach proposed by Walton and Braun (1986) is based on a bilinear law for normal contact of spheres, Figure 2b. The equations for each part of the bilinear relationship are:

$$P = K_1 \alpha \quad \text{for loading,} \qquad [10]$$
$$P = K_2(\alpha - \alpha_0) \quad \text{for unloading,}$$

Here, K_1 and K_2 are the slopes of the straight lines representing the loading and unloading paths, and α_0 is the residual displacement after complete unloading.

Thornton (1997) proposes a model that follows Hertz theory while the distribution of normal stress on the contact area is below a yield stress σ_Y. Afterwards, Thornton (1997) assumes a constant stress distribution and a linear relationship between the normal displacement α and the normal contact force P. During unloading the model follows the Hertz law but uses a larger radius R_p^* of relative contact curvature due to the irreversible plastic strains, Figure 2c. The contact yield

stress σ_Y is the maximum normal pressure on the contact area (p_0) at yielding; using the Von Mises criterion, Thornton (1997) proposes σ_Y =1.61σ_c where σ_c is the yield stress of the sphere material, Figure 2a.

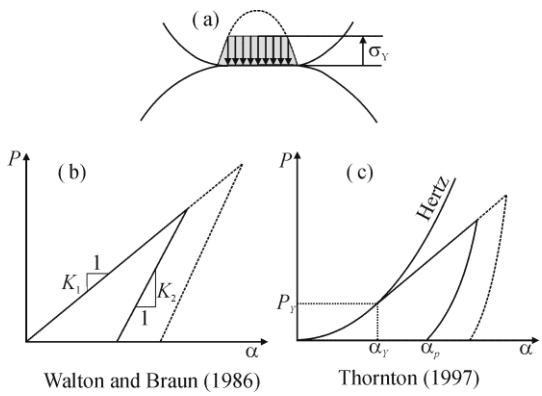

Figure 2. Plastic stress distribution, relationships between P and α.

Vu-Quoc and Zhang (1999), using the formalism of the continuum theory of elastoplasticity proposes an additive decomposition of the contact radius a^{ep} as follows:

$$a^{ep} = a^p + a^e \qquad [11]$$

where a_e is the elastic part depending on Hertz theory and a_p is the plastic part of the contact radius. This decomposition is based on the permanent deformation that remains on the contact surface after complete unloading; this residual contact radius is a_{res}, see Figure 3.

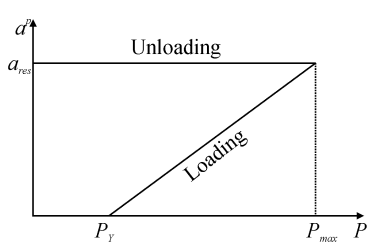

Figure 3. α^p–P curve for normal contact between elastic–perfectly plastic spheres, Vu-Quoc and Zhang (1999).

After numerous FEA results, Vu-Quoc and Zhang (1999) proposes the following relationship for the plastic contact radius:

$$a_p = C_a \langle P - P_Y \rangle \qquad \text{for loading,} \qquad [12]$$

$$a_p = C_a \langle P_{\max} - P_Y \rangle \qquad \text{for unloading,}$$

Where Ca is a constant and the brackets $\langle\ \rangle$ are the MacCauley operator defined as follows:

$$\langle x \rangle = 0 \qquad \text{for} \qquad x \le 0\text{, and} \qquad [13]$$

$$\langle x \rangle = 0 \qquad \text{for} \qquad x > 0$$

In addition Vu-Quoc and Zhang (1999) remarks that when plastic strains appears in the contact between particles flattens, then the effect of irreversible plastic strains increases the radius of curvature compared with the original curvature, i.e. $R_p > R$, see Figure 4. The following linear relationship was proposed by Vu-Quoc and Zhang (1999) to obtain the plastic radius of curvature:

$$R_p = C_R R \qquad [14]$$

$$C_R = 1 \qquad \text{for} \qquad P \le P_Y\text{, and} \qquad [15]$$

$$C_R = 1 + K_c \langle P - P_Y \rangle \qquad \text{for} \qquad P > P_Y$$

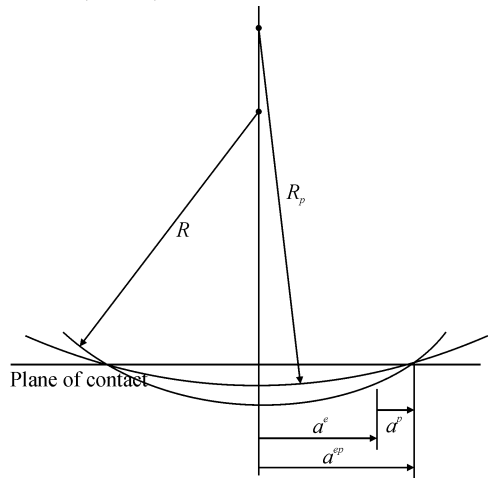

Figure 4. Plastic deformation increases the radius of relative contact curvature, Vu-Quoc and Zhang (1999).

Where K_c is a constant, the previous assumptions allows expanding Hertz theory to the elastoplastic range. The incipient yield normal force P_Y is obtained by:

$$P_Y = \frac{\pi^3 R^2 (1-\nu^2)^2}{6E^2} \left[A_Y(\nu)\sigma_c \right]^3 \qquad [16]$$

where $A_Y(\nu)$ is a scalar that depends on the Poisson's ratio, for ν=0.3 $A_Y(\nu)$=1.61. At the yielding point, the contact area radius a_Y and the normal displacement α_Y are:

$$a_Y = \left[\frac{3P_Y R(1-\nu^2)}{4E} \right]^{1/3}\text{, and } \alpha_Y = \frac{a_Y^2}{R} \qquad [17]$$

The relationship between load and displacement between spheres is given by the following relationship, details about its derivation is given in Vu-Quoc and Zhang (1999).

$$(P - P_Y) + c_1 P^{1/3} - \frac{1}{C_a} \left\{ 1 + K_c (P - P_Y) \right\} R\alpha^{3/2} = 0\text{,} \qquad [18]$$

$$c_1 = \frac{1}{C_a}\left[\frac{3R(1-\nu^2)}{4E}\right]^{1/3} \qquad [19]$$

2.3 Effect of suction of the strength of particles

Researches about crushing of rock fills carried out at Barcelona proved that subcritical crack propagation within rocks provides useful explanation for the effect of suction on the fracture propagation within rocks, Alonso and Oldecop (2000), Chavez and Alonso (2003), Oldecop (2000), Oldecop and Alonso (2001, 2003).

These researches are based on the classical theory of fracture mechanics which relates crack propagation with the stress intensity factor (K) that depends of the geometry of the problem, the loading mode and of the intensity of the applied stress.

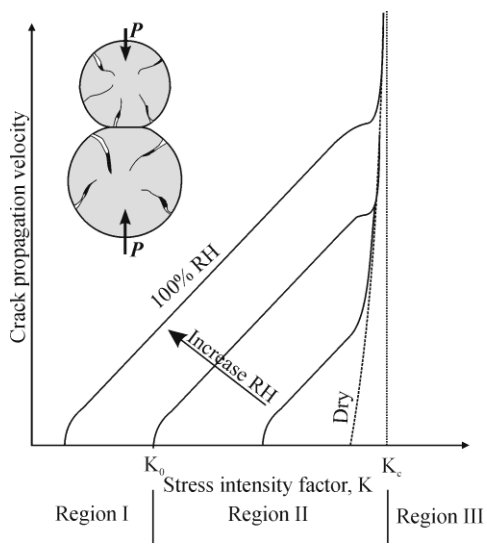

Figure 5. Schematic subcritical crack growth curves and conceptual model (Alonso & Oldecop,2000).

The subcritical crack growth mechanism proposed by Alonso & Oldecop (2000) explains why both time and strains affect the strength of rock fill particles but can be directly generalized to particles in a granular material. In fact particles forming part of a granular material also have micro and macro-cracks that can propagate due to the interaction of load and water effects.

The schematic representation of Figure 5, proposed by Alonso and Oldecop (2000), describes the effect of relative humidity (and therefore suction) on the strength of particles. Using this framework, the stress intensity factor axis was divided into three regions. Cracks lying in region I ($K<K_0$) do not propagate at all. If a load increment is then applied, the K values will move along the K axis.

Cracks falling in region III where the stress intensity factor is larger than the fracture toughness, Kc fails instantaneously, finally cracks falling in region II grows with a finite value of propagation velocity. According to this model Alonso and Oldecop (2000) concludes that the key parameter which controls the influence of water in the mechanical behaviour of particles is the relative humidity.

3 EXPERIMENTAL WORK

The possibility of applying the theories described above in granular materials was verified experimentally. Spheres of different size, strength and suction were prepared. Afterwards their stress-strain behaviour, the strength and the grain size distribution after failure were studied. The following paragraphs describe the experimental setup to measure these behaviour characteristics.

3.1 Production of the spherical particles

To carry out a parametric study assessing the effect of different parameters like suction, strength and size of the particles in the overall behaviour of granular materials it is crucial to have a method to produce particles in a reproducible way. Producing artificial spherical particles is a method that allows controlling its size, strength, elastic properties, and suction.

The spherical particles were built using mortar of different strength; the characteristics of the mortar were chose to fit the behaviour of sandstones used as a granular material for pavements in Bogotá. The three different strength of the mortar were: 12 MPa, 20 MPa, and 28 MPa and the three different diameters were 15mm, 20mm and 25mm.

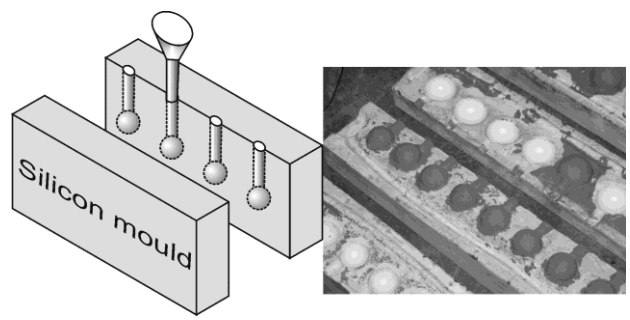

Figure 6. Silicon mould to prepare spherical particles.

The spherical particles were prepared in a silicon mould that allows obtaining 10 particles of the same size for each batch, Figure 6. Particles remain in the mould during one day and then there are removed and immersed in water during 28 days. Afterwards the particles are conditioned at different suction pressures using vapor equilibrium method.

Moreover, samples of mortar were built with cylindrical shape to measure its elastic properties and strength, Table 1 shows the result of these measures.

Table 1. Characteristics of mortar mixtures.

Mixture	E (MPa)	σ_c (MPa)
Mixture 1	1304	15.3
Mixture 2	2620	21.7
Mixture 3	2800	28.2

E: Young modulus; σ_c, saturated strength.

3.2 Suction conditioning

As described, in the theoretical framework of this paper, suction has an important role in the crack propagation in granular materials. To study this effect the spherical particles were conditioned at different suction pressures using the vapour equilibrium method.

The particles were conditioned using four different relative humilities, RH, that were obtained using different concentrations of sulphuric acid and distilled water, see Table 2.

Table 2. Acid concentrations and suction.

Acid concentration g/cm^3	RH	Suction (MPa)
1.05	97.73	3.16
1.205	79.51	31.62
1.344	48.43	100
1.578	10.10	316.23

Figure 7. Conditioning suction in a desiccator.

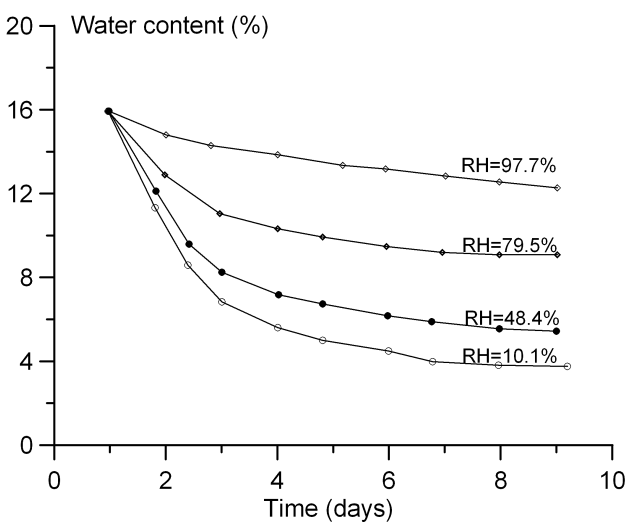

Figure 8. Water content equilibrium during desiccation.

Several spherical particles were conditioned in a desiccator and its weight was monitored up to constant weight, Figures 7 and 8.

Once the equilibrium is achieved the weight of the particles is measured and its water content is calculated. Figure 9 shows the water retention curve of the particles measured using the procedure described previously.

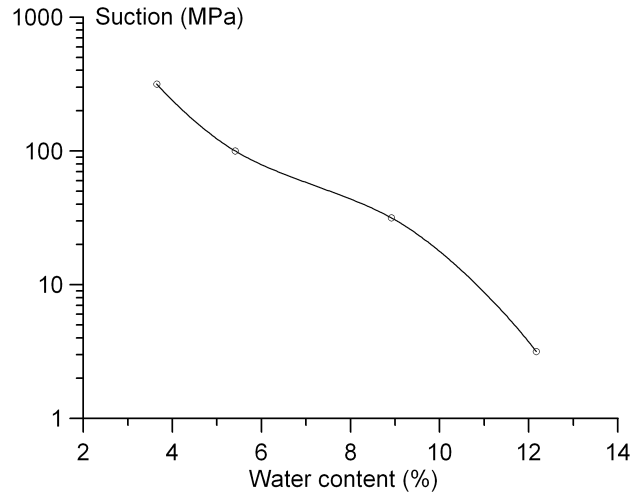

Figure 9. Water retention curve for the spherical particles.

3.3 Experimental setup

The spherical particles were tested under compression loading using a device that allows recording load and displacement under compression. This device has the following components, Figures 10 and 11:

- A set of cylindrical moulds having internal diameter 1/10mm larger than the size of the spheres, in addition the moulds have two windows that allows locating the LVDT references
- Each mould has two rubber cushions located up and bottom of the set of two spheres
- A set of two LVDTs to measure the relative displacement between spheres
- A cell to measure compression load.

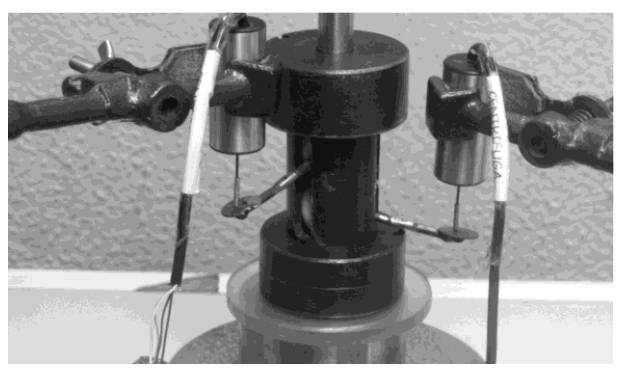

Figure 10. Experimental setup.

The conception of the mould forbids rolling of particles as the spheres are precisely confined in the mould and the rubber cushion provides friction in antagonism to rolling. On the other hand the rubber cushion allows smooth load transmission at the upper and lower part of the set of particles, this mean that the main stress concentration takes place at the contact between particles.

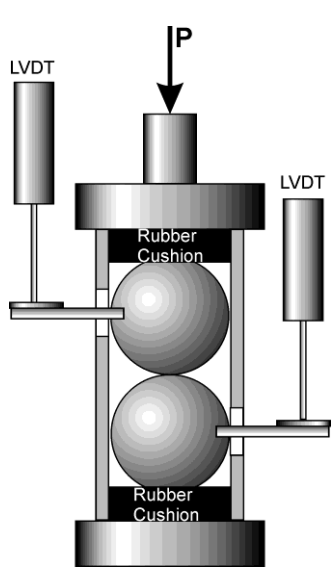

Figure 10. Layout of the experimental setup.

4 RESULTS

The tests allow analysing different aspects of the behaviour of particles under compression loads. Three different aspects are analysed in this paper: load-deformation behaviour under monotonic and cyclic loading, strength and the grain size distribution after breakdown. However this paper presents only typical results, a detailed analysis involving all the parameters will be presented in a longer paper.

4.1 Load – deformation behaviour

As an example, Figure 11 presents the load-deformation curve corresponding to a set of particles having 15 mm diameter and conditioned at RH=10.1. This curve reveals that the experimental results show less rigid behaviour than the elastic behaviour of the Hertz theory. This is a clear evidence of the plastic strains appearing in the contact between particles at early loads. On the other hand, the Thornton (1997) approach leads to a softer contact between particles compared with the experimental results.

As shown in Figure 11, the elastoplastic approach proposed by Vu-Quoc and Zhang (1999) allows fitting with good accuracy the experimental results, this approach was used to analyse the contact behaviour under cyclic loading.

Figure 12 presents the experimental results of a set of spheres having the same characteristics than those presented in Figure 11. The elastoplastic approach of Vu-Quoc and Zhang (1999) allows fitting the experimental results but only on the loading stage; during unloading the load on the experimental results decrease more rapidly than the decrease of the theoretical model. This discrepancy suggests that during unloading it is necessary to adjust Hertz theory in a similar way than during loading.

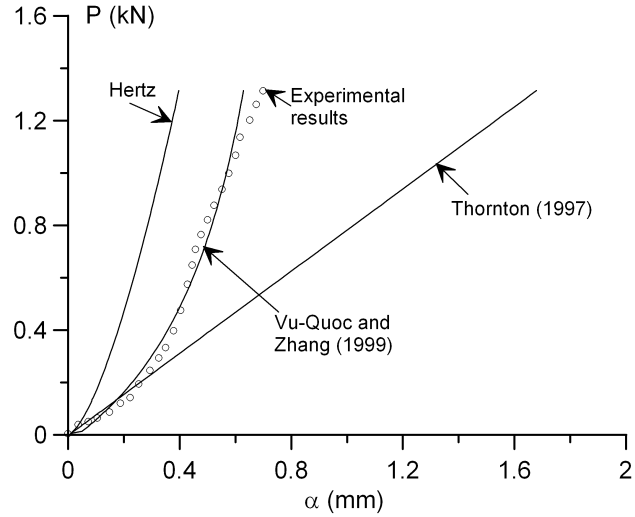

Figure 11. Monotonic load-deformation curve for 15 mm particles and RH=10.1%.

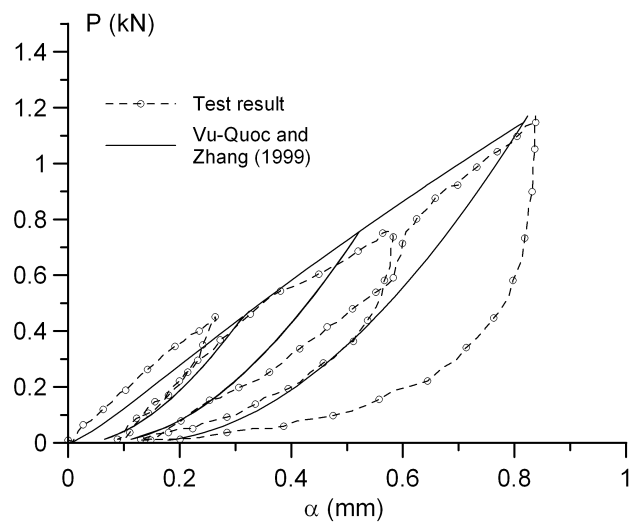

Figure 12. Cyclic load-deformation curve for 15 mm particles and RH=10.1%.

4.2 Strength of particles

Figure 13 presents the limit compression load at failure upon suction and particle size. As observed, the limit load increases with suction this behaviour is in agreement with the subcritical crack growth mechanism proposed by Alonso & Oldecop (2000).

To analyze the effect of the size of the particles it is useful to calculate the characteristic strength defined by Lee (1992) as follows:

$$\sigma = \frac{P}{D^2} \qquad [20]$$

Where P is the point load at failure and D is the particle diameter. Lee (1992) also proposes a potential equation to describe the evolution of the strength of particles upon its size:

$$\sigma \propto D^b \qquad [21]$$

The parameter *b* is measured by Lee (1992) is negative that means that the strength of the particles reduces as its size increases.

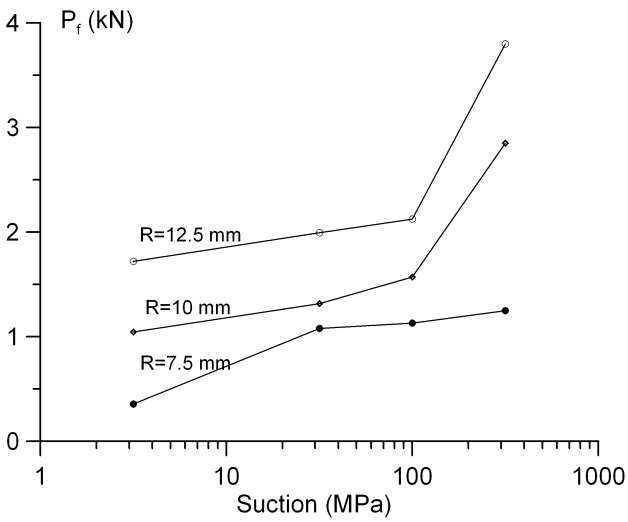

Figure 13. Limit compression load for particles of different size and suction.

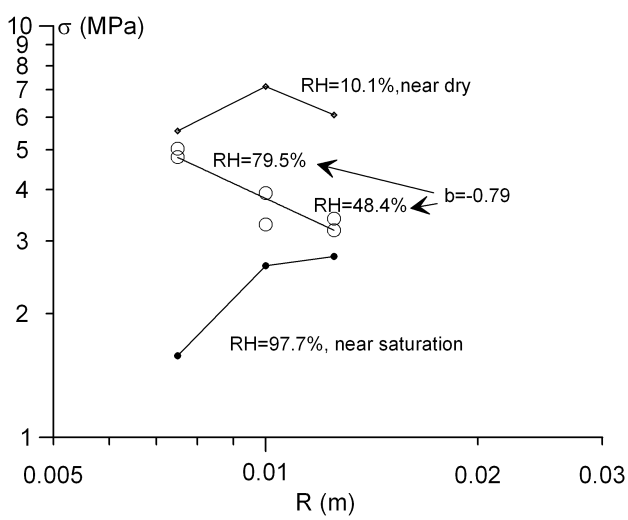

Figure 14. Limit compression strength for particles of different size and suction.

Figure 14 presents the strength of the particles according with the strength defined by Lee (1992); this figure shows that the strength of the particles conditioned to intermediate relative humidity have a good agreement with the decreasing potential law. However for particles that approaches the dry or the saturated states the behavior is different: almost constant strength for dry state, and strength increasing with the size for particles near saturation. The source of this discrepancy requires further research.

4.3 Grain size distribution after crushing

One of the key points in the analysis of granular materials under crushing is the grain size distribution after particle breaking. This aspect was performed following a sieve analysis after particle failure, Figure 15.

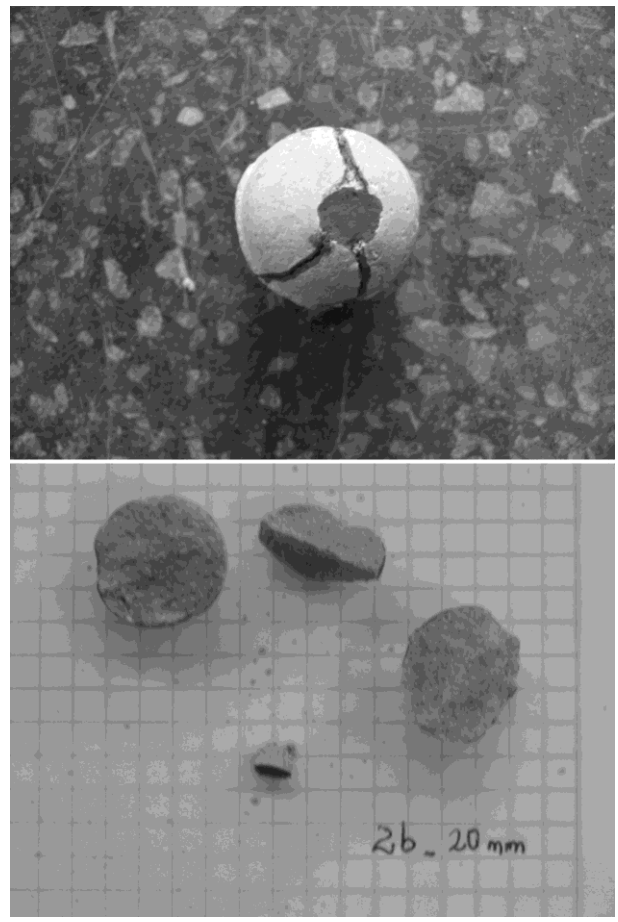

Figure 15. Size of particles after failure.

Figure 16 shows the range of grain size distribution after crushing of particles, this range is defined as a function of the relationship between the size of the sub particle and the original size.

As observed in Figure 16 the particles after crushing can be grouped in two sets: the first family is made by most of the sub-particles that have a size larger than 30% of its original size. On the other hand a second family of crushed particles has a size lower than 74 μm, these particles are probably coming from the failure surfaces within the particles.

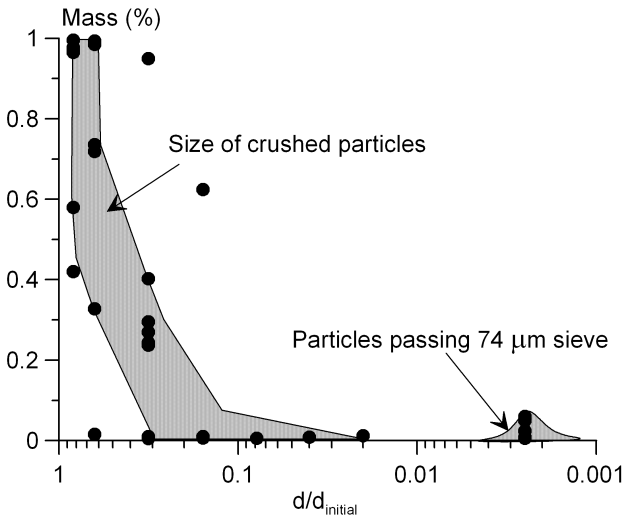

Figure 16. Grain size distribution of crushed particles.

5 CONCLUSIONS

This paper presents a research about the behaviour of spherical particles under compression. The effect of size and suction is studied. The following conclusions can be addressed from the experimental results:

- Hertz theory is not a useful theory to describe the behavior of the contact of particles since plastic strains appears at low loads.
- Using elastoplastic theories it is possible to fit in a better way the loading of spherical particles but modeling unloading requires the development of further theories.
- The effect of suction on the strength of particles agrees with the subcritical crack growth propagation proposed by Alonso and Oldecop (2000). However the effect of the size is only clear for intermediate relative humidity.
- The results of grain size distribution after crushing provides a useful data to model granular material under crushing.

REFERENCES

Allersma H.G.B. (1987). Optical analysis of stress and strain in photoelastic particle assemblies. PhD, Delft Technical University.

Allersma, H.G.B. 2001. Optical analysis of stress and strain around a penetrating probe in a granular medium. Powder & Grains, Sendai,Swets & Zeitlinger, Lisse, p.85-88

Alonso, E.E. & L.A. Oldecop (2000). Fundamentals of rockfill collapse. 1st Asian Conference on Unsat. Soils. Singapore.

Cundall, P.A., Strack,O.D.L, (1979).:Adiscrete numerical model for granular assemblies. Geotechnique 29(1), 47–65.

Chávez and Alonso, E.E. (2003) A constitutive model for crushed granular aggregates which includes suction effects. Soils and Foundations, Vol. 43, No. 4, 215-228.

Cheng,Y.P.,Nakata,Y., Bolton, (2003) M.D.:Discrete element simulation of crushable soil. Geotechnique 53(7), 633–641

Dantu, P. 1957. Contribution l'étude méchanique et géométrique des milieux pulvérulents. Proc. Int. Conf. Soil Mech. & Found. Eng., London, Vol.1:144-148.

Drescher A. (1976). “An experimental investigation of flow rules for granular materials using optically sensitive glass particles”, Geotechnique 26(4), 591-601.

Drescher, A., De Josselin de Jong, G., (1972). “Photoelastic verification of a mechanical model for the flow of a granular material”. J.Mech.Phys.Solids 20, 337-351.

Harireche, O., McDowell, G.R. (2003): Discrete element modelling of cyclic loading of crushable aggregates. Granular Matter 5, 147– 151.

Hertz, H. 1882 ¨Uber die Ber¨uhrung fester elastischer K¨orper (On the contact of elastic solids). J. Reine Angewandte Math. 92, 156–171.

Jensen, R.P., Plesha, M.E., Edil, T.B., Bosscher, P.J., Kahla, N.B. (2001): DEM simulation of particle damage in granular media – structure interfaces. Int J Geomech 1(1), 21–39.

Lee, D. M. (1992). "The angles of friction of granular fills," Ph.D. dissertation, University of Cambridge.

Lobo-Guerrero S., Vallejo L.E., (2006). Discrete element method analysis of railtrack ballast degradation during cyclic loading, Granular Matter (2006) 8: 195–204

Lobo-Guerrero, S., Vallejo, L.E. (2005a): Crushing a weak granular material: experimental numerical analyses. Geotechnique 55(3), 245– 249.

Lobo-Guerrero, S., Vallejo, L.E. (2005b): Analysis of crushing of granular material under isotropic and biaxial stress conditions. Soils Foundations 45(4), 79–88.

McDowell, G.R., Harireche, O.: Discrete element modelling of yielding and normal compression of sand. Geotechnique 52(4), 299–304 (2002)

Oldecop, L. (2000). “Compresibilidad de escolleras. Influencia de la humedad”. PhD. Thesis. UPC.

Oldecop, L. and Alonso EE (2001). ”A model for rockfill compressibility”. Géotechnique 51(2), pp. 127-140.

Oldecop, L.A. and Alonso, E.E. (2003), “Suction effects on rockfill compressibility” Géotechnique, Vol. 53, pp. 289-292.

Thornton, C. 1997 Coefficient of restitution for collinear collisions of elastic perfectly plastic spheres. ASME JlAppl . Mech. 64, 383–386.

Vu-Quoc L., Zhang, X., (1999). An elastoplastic contact force–displacement model in the normal direction: displacement-driven version. Proc. R. Soc. Lond. A 455, 4013–4044

Walton, O. R. & Braun, R. L. 1986 Viscosity, granular-temperature, and stress calculations for shearing assemblies of inelastic, frictional disks. J. Rheology 30, 949–980.